POLİTEKNİK DERGİSİ

JOURNAL of POLYTECHNIC

ISSN: 1302-0900 (PRINT), ISSN: 2147-9429 (ONLINE)
URL: http://dergipark.gov.tr/politeknik

Lattice parameters a-, c-, strain-stress analysis and thermal expansion coefficient of InGaN/GaN solar cell structures grown by MOCVD

MOCVD ile büyütülen InGaN/GaN güneş hücresi yapısının a-,c- örgü parametreleri, zorlama-gerilme analizi ve termal genleşme katsayısı

***Yazar(lar) (Author(s))**: A.Kürşat BİLGİLİ[1], Ömer AKPINAR[2], Gürkan KURTULUŞ[3], M.Kemal ÖZTÜRK[4], Süleyman ÖZÇELİK[5], Ekmel ÖZBAY[6]*

ORCID[1]: 0000-0003-3420-4936

ORCID[2]: 0000-0002-5172-8283

ORCID[3]: 0000-0002-3769-6094

ORCID[4]: 0000-0002-8508-5714

ORCID[5]: 0000-0002-3761-3711

ORCID[6]: 0000-0003-2953-1828

Bu makaleye şu şekilde atıfta bulunabilirsiniz(To cite to this article): Bilgili A.K., Akpinar O., Kurtulus G., Ozturk M.K., Ozcelik S. and Ozbay E., “Lattice parameters a-, c-, strain- stress analysis and thermal expansion coefficient of InGaN/GaN solar cell structures grown by MOCVD”, ***Journal of Polytechnic***, 22(1): 33-39, (2019).

Erişim linki (To link to this article): http://dergipark.gov.tr/politeknik/archive

DOI: 10.2339/politeknik.403978

Lattice Parameters a-, c-, Strain-Stress Analysis and Thermal Expansion Coefficient of InGaN/GaN Solar Cell Structures Grown by MOCVD

Research Article / Araştırma Makalesi

A.Kursat BILGILI[1*] , Omer AKPINAR[1,2], Gurkan KURTULUS[2], M. Kemal OZTURK[1,2], Suleyman OZCELIK[1,2], Ekmel OZBAY[3]

[1]Department of Physics, Gazi University, 06500 Ankara, Turkey
[2]Photonics Research Center, Gazi University, 06500 Ankara, Turkey
[3]Nanotechnology Research Center, Bilkent University, 06800 Ankara, Turkey

(Received : 20.10.2017 ; Accepted : 26.02.2018)

ABSTRACT

Structural properties of InGaN/GaN solar cells (SCs) grown by metal organic chemical vapor deposition (MOCVD) technique are investigated by high resolution X-ray diffraction (HR-XRD) method. It is noticed that a- and c- lattice parameters of the structures showed small differences according to examined (hkl) planes. Fault percentage of the a- and c- lattice parameters are also calculated. It is seen that fault percentage is smaller than %2 for all samples. Investigations have been made for three different samples. Differences in crystal quality caused by growth conditions are seen in all three samples. At the same time, properties such as crystal size, strain and stress are determined. During determination of stress, two different methods including elastic constants, Young module and Poisson ratio are used. Results gained from these two methods are compared with each other. Thermal expansion coefficients of InGaN are calculated for (002), (004), (006) and (121) planes for 100 °C temperature difference (300-400 °C). It is seen that peak positions gained from HR-XRD are nearly the same with the ones in database. All the results obtained from calculations are given in tables in the following sections of this article. It can be seen that all these results are in accordance with previous works done by different authors and with the real values.

Keywords: Lattice, crystal, GaN, InGaN, MQW, thermal.

MOCVD ile Büyütülen InGaN/GaN Güneş Hücresi Yapısının a-,c- Örgü Parametreleri, Zorlama-Gerilme Analizi ve Termal Genleşme Katsayısı

ÖZ

Metal organik kimyasal buhar biriktirme (MOCVD) tekniği ile büyütülen InGaN/GaN güneş hücrelerinin (SC) yapısal özellikleri yüksek çözünürlüklü X-ışını kırınımı (HR-XRD) yöntemi ile araştırılmıştır. Yapıların a- ve c- örgü parametrelerinin incelenen (hkl) düzlemlere göre küçük farklılıklar gösterdikleri dikkat çekmektedir. a- ve c- örgü parametrelerinin hata yüzdeleri hesaplandı. Tüm numuneler için hata yüzdesinin %2'den küçük olduğu görülmektedir. Üç farklı numune için araştırmalar yapılmıştır. Her üç numunede de büyüme koşullarından kaynaklanan kristal kalitesinde farklılıklar görülür. Aynı zamanda Kristal boyutu, zorlama ve gerilme gibi özellikleri de belirlendi. Gerilmenin belirlenmesinde elastik sabitler, Young modülü ve Poisson oranı olmak üzere farklı yöntemler kullanıldı. Yöntemlerden elde edilen sonuçlar birbirleriyle karşılaştırılmıştır. InGaN'ın termal genleşme katsayıları 100°C sıcaklık farkı (300-400 °C) için (002), (004), (006) ve (121) düzlemleri için hesaplandı. HR-XRD'den elde edilen pik pozisyonlarının veri tabanlarındaki (database) pik pozisyonlarıyla neredeyse aynı olduğu görülmektedir. Hesaplamalardan elde edilen tüm sonuçlar bu çalışmanın bölümlerinde yer alan tablolarda verilmektedir. Bütün bu sonuçların farklı yazarlar tarafından yapılmış önceki eserlere ve gerçek değerlere uygun olduğu görülmektedir.

Anahtar Kelimeler: Kafes, kristal, GaN, InGaN, MQW, termal.

1. INTRODUCTION

AlN, GaN, InN and III-V group nitrite material system which include their alloys is a wide research area because of applications such as solar cells (SCs), laser diodes and photo censors [1]. InN alloy with a band gap of 0.65 eV and InGaN with a band gap reaching from infrared region to ultraviolet region are common materials to be investigated [2-3]. This direct and wide band gap spectrum makes the InGaN material system applicable for photovoltaic device design [4-5]. GaInP-GaInAs-Ge which has three junctions has a performance of %39, but structures containing InGaN has better efficiency [6-7].

SC with InGaN active layer is an important nano-technology device which takes attention in recent years. Especially sapphire (Al_2O_3) which is used as wafer and

* *Sorumlu yazar (Corresponding Author)*
e-posta : sunkurt4@gmail.com

active layer over it, have a great lattice mismatch. This situation causes cracks and dislocations at active layer. GaN nucleation and buffer layers limits the passing of dislocations to active layers. GaN is a useful buffer material because of its accepted lattice mismatch and relaxation values for active layers such as $In_xGa_{1-x}N$ [8]. In this study, lattice parameters a- and c, stress values, crystal size are investigated with different methods and compared with each other. Fault percentage in lattice parameters and precise a- and c values are determined. Many different studies are made for the structural properties mentioned above. For example; Birks et al, investigated crystal size of carbonate and MgO particles by x-ray line broadening, they noticed that particle size could not be determined unless the two maxima of the distribution curve were completely resolved [9]. Delhez et.al investigated the methods for determining crystallite size from x-ray diffraction line broadening. They commented on size broadening and strain broadening [10].

2. EXPERİMENTAL DETAİLS

InGaN1/InGaN2/GaN solar cell structures are deposited on c-oriented Al_2O_3 with MOCVD growth technique. Before growth of epitaxial film, in order to remove impurities on the surface, samples are cleaned at 1100 ºC temperature in H_2 atmosphere for 10 minutes. After this cleaning procedure, firstly GaN nucleation layer is deposited on Al_2O_3 at 575 ºC. During growth, trimethyl gallium (TMGa) flux ratio is set as 10 sccm, NH_3 flux ratio is set as 1500 sccm and growth pressure is set as 200 mbar. The thickness of this seed layer is 10 nm. After growth of this nucleation layer, GaN buffer layer is deposited on it at 1070 ºC. During the growth of this buffer layer flux ratios of TMGa and NH_3 are set as 15 sccm and 1800 sccm respectively. The growth pressure of this buffer layer is set as 200 mbar. The thickness of this buffer layer is 1.6 µm. Growth procedure continued with turning on the SiH_4 source. With the help of this SiH_4 source n-type GaN layer is obtained. In MOCVD operation SiH_4 source has dilute property. The flux ratio of this source is 10 sccm. $In_xGa_{1-x}N$ active layers are deposited at 745-760 ºC temperatures at 75 sccm In flux ratio. Active layers are deposited between 1.9 µm thick n-type GaN and p-type InGaN layers.

p-type (p^+) InGaN layer is deposited with Mg source. The flux ratio of this source is 35 sccm. During the growth of this InGaN layer, the sources for other layers are kept at off position. In order to make more doping the flux ratio of Mg source is set as 40 sccm in InGaN layers used as active layers.

3. RESULTS

In this part of the study, with the analysis of the HR-XRD measurement of InGaN SC structures, lattice parameters, stress, strain, crystal size and thermal expansion coefficient of InGaN layer are determined with different methods and related data are given in tables. Some of the results gained from different methods are compared with each other.

3.1 XRD

Nitrite based alloys and compounds such as GaN and InGaN has hexagonal structure. Broadening of HR-XRD rocking scan curves in such layers comes out by variation of tilt and twist angles and lateral crystal length parallel to wafer surface. Full width at half maximum (FWHM) of HR-XRD-omega peaks for GaN and InGaN layers are given in table 1. These peaks are shown in figure 1. When the measured values are compared, it can be seen that FWHM values for GaN layers in all three samples are approximately the same for (00l, l = 1, 2, 4, 6) planes. This result indicates that growth conditions for all three samples are similar to each other.

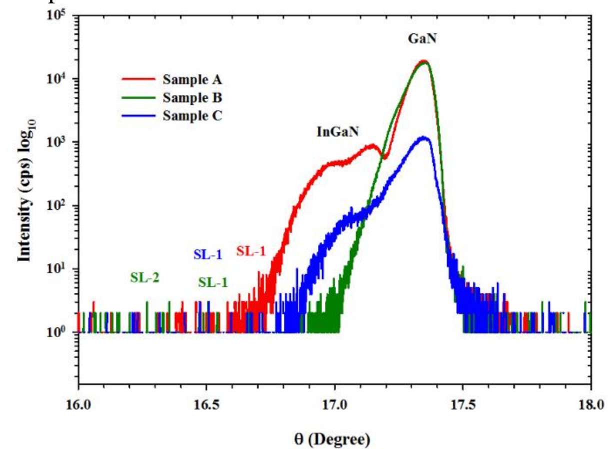

Figure 1. θ versus intensity plots of S.A, B and C.

InGaN layer in S.A has lower FWHM values than samples B and C. This means that InGaN layer in S.A has a better crystal quality.

Table 1. a) Peak positions of GaN layer for (101), (102), (121) planes, b) Peak positions of InGaN layer for (002), (004), (006), (102) planes

a)

	S.A	S.B	S.C
(hkl)	*Omega(^{O})*	*Omega(^{O})*	*Omega(^{O})*
101	18.468	18.259	18.297
102	24.052	24.075	24.095
121	48.904	48.887	48.903

b)

	S.A	S.B	S.C
(hkl)	*Omega*	*Omega*	*Omega*
002	16.92	17.128	17.025
004	35.723	36.013	35.735
006	61.935	61.771	62.576
102	23.854	18.162	23.87

In figure.1 it can be seen that on the left of GaN top peak, InGaN1 and InGaN2 peaks are not fully distorted. On the left of these InGaN peaks there can be seen a slight satellite peak. This satellite peak contains information

Table 3. Lattice Parameters for GaN

	GaN					
	S.A		S.B		S.C	
(hkl)	*c(Å)*	*a(Å)*	*c(Å)*	*a(Å)*	*c(Å)*	*a(Å)*
(101)	0.517	0.316	0.516	0.320	0.515	0.319
(102)	0.518	0.313	0.510	0.313	0.510	0.313
(121)	0.517	0.316	0.507	0.317	0.507	0.316

Table 4. Lattice Parameters for InGaN

S.A						
(hkl)	*a(certain)(nm)*	*a(calculated)(nm)*	*%Fault(a)*	*c(certain)(nm)*	*c(calculated)(nm)*	*%Fault(c)*
(101)	0.322	0.320	0.60	0.528	0.527	0.19
(102)	0.322	0.318	1.41	0.528	0.527	0.01
(121)	0.322	0.317	1.72	0.528	0.527	0.09
S.B						
(hkl)	*a(certain)(nm)*	*a(calculated)(nm)*	*%Fault(a)*	*c(certain)(nm)*	*c(calculated)(nm)*	*%Fault(c)*
(101)	0.323	0.324	0.39	0.531	0.529	0.34
(102)	0.323	0.319	1.40	0.531	0.525	1.10
(121)	0.323	0.322	0.50	0.531	0.522	1.63
S.C						
(hkl)	*a(certain)(nm)*	*a(calculated)(nm)*	*%Fault(a)*	*c(certain)(nm)*	*c(calculated)(nm)*	*%Fault(c)*
(101)	0.320	0.321	0.24	0.531	0.526	0.97
(102)	0.320	0.315	1.64	0.531	0.522	1.68
(121)	0.320	0.318	0.58	0.531	0.520	2.21

Table 5. Precise a- and c values for GaN and InGaN layers

	GaN	InGaN
	Precise a(nm)	*Precise c(nm)*
S.A	0.316	0.518
S.B	0.315	0.504
S.C	0.315	0.504

about quantum well (QW) thickness. The situation is the same for S.B but on the left of GaN top peak InGaN peaks are together and there are two satellite peaks. For S.C InGaN peaks are again on the left of GaN top peak. They are not clearly distorted. As seen in figure 1 best crystal quality is in S.A. This may be because of more optimized growth conditions for S.A.

3.2 Lattice Parameters

In HR-XRD technique in order to separate $K_{\alpha 1}$ and $K_{\alpha 2}$ rays in parallel beam and to eliminate $K_{\alpha 2}$, Ge 022 (+,-,-,+) monochromator is used together with Goebel mirror. With symmetric and asymmetric reflections, Bragg angle θ and lattice slope angle τ can be calculated with the following expressions; $\theta = (\theta_+ + \theta_-)/2$ and $\tau = (\theta_+ - \theta_-)/2$[11]. a- and c- lattice parameters of disordered InGaN hexagonal unit cell can be calculated by appropriate (hkl) reflection angles. In table. 2, values of τ angles corresponding some planes can be seen.

Table 2. τ angles corresponding to (101), (102), (106), (121) planes

(hkl)	*τ(degree)*
101	61.9599
102	43.1913
106	17.3763
121	78.6181

Lattice parameters of InGaN layer can be found by using Vegard's law. It is calculated as x times InN lattice parameter and (1-x) times GaN real lattice parameter. Here x is the In content in samples calculated again by Vegard's law.

$$a_{InGaN} = (x)a_{InN} + (1-x)a_{GaN} \tag{1}$$

$$c_{InGaN} = (x)c_{InN} + (1-x)c_{GaN} \tag{2}$$

If we use values gained from equation (3) and (4) instead of last terms in equations (1) and (2) we reach to experimental values. If we use real values in literature we reach to certain values. We can make fault calculation by using these two results.

By taking cubic system as reference, in order to gain a- and c- lattice parameters for GaN layer we used sinτ and cosτ modification integers in equation (3) and (4).

$$c = \frac{\lambda l}{2\sin\theta\cos\tau} \tag{3}$$

$$a = \frac{\lambda\sqrt{4/3}\sqrt{h^2 + hk + k^2}}{2\sin\theta\sin\tau} \tag{4}$$

a- and c lattice parameters mentioned above are given in table. 3, 4 and 5 for GaN and InGaN layers. In addition

to these we can find precise a- and c values by the help of $\cos^2\theta/\sin\theta$ versus a- and c measured values plot in figure. 2. Y axis intercept of this plot gives us precise a- and c values.

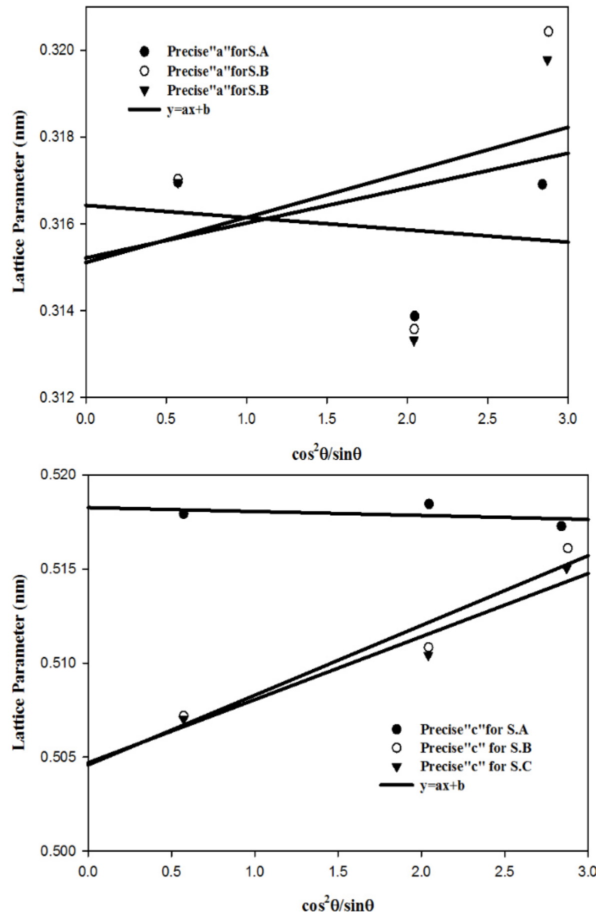

Figure 2. $\cos^2\theta/\sin\theta$ versus lattice parameters plots of S.A, B and C for GaN layer.

3.3 Strain, Stress and Crystal Size

It is possible to find stress from strain measurements. If there is a rotationally symmetric strain position, stress can be found from strain [12]. The relation of biaxial strain ε_a with stress is given in equation (5).

$$\varepsilon_a = \frac{\sigma^*(1-\upsilon)}{E} \tag{5}$$

Here, ε_a is strain, σ^* is stress, υ is Poisson's ratio and E is Young modulus [13]. Stress by the help of elastic constants can be found with equation (6).

$$\sigma^* = (c_{11} + c_{12} - \frac{2c_{13}^{\ 2}}{c_{33}})\varepsilon_a \ [13] \tag{6}$$

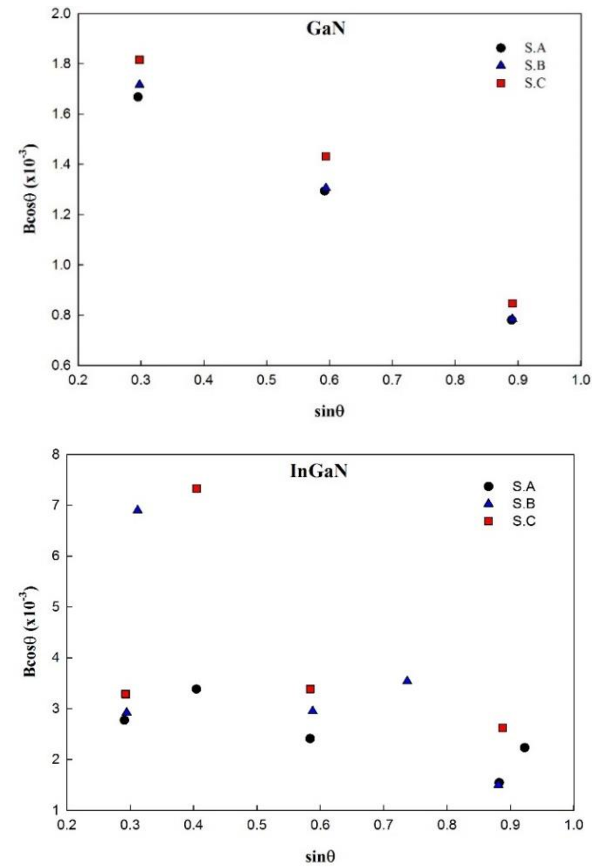

Figure 3. $\sin\theta$ versus $\beta\cos\theta$ plots of S.A, B and C for GaN and InGaN layers

Strain value in equation (5) (ε_a) can be found by $\sin\theta$ versus $\beta\cos\theta$ plot. Here β is the modified FWHM value. This plot is shown in figure 3. The slope of this plot gives us ε_a value. Y axis intercept of this plot gives us $k\lambda/L$. In general k is taken as 1. Here L is the crystal size [14].

Table 7(d). a- and c lattice parameters in Å for (121) plane for S.A, B, C at different temperature

	S.A		**S.B**		**S.C**	
Temperature(^{o}C)	*a*	*c*	*a*	*c*	*a*	*c*
300	3.371	5.275	3.220	5.229	3.187	5.201
350	3.171	5.275	3.219	5.227	3.185	5.198
400	3.173	5.277	3.222	5.232	3.189	5.205
450	3.173	5.278	3.221	5.230	3.190	5.207

Stress is found from equation (5) and (6). Both results are in accordance with each other. Results are summarized in table 6. In this study Young modulus is taken as 305, Poisson's ratio is taken as 0.183 and elastic constants c_{11}, c_{12}, c_{13}, c_{33} are taken as 390, 145, 106, 398 GPa

Table 6. Crystal size, strain and stress values for GaN layers.

	S.A	S.B	S.C
Strain (GPa)	-0.0015	-0.0016	-0.0016
Crystal Size (nm)	73.36	70.03	66.98
Stress by Young modulus (GPa)	-0.5599	-0.5973	-0.5973
Stress by elastic constants (GPa)	-0.7178	-0.7656	-0.7656

3.4 Thermal Expansion Coefficients

Thermal expansion coefficient of a solid is the variation in length with a change of 1 ºC in temperature. As known by thermodynamics every matter expands when heated because the energy of atoms increase and they vibrate faster. As a result of this they move away from each other but in very small scales. The situation is the same for solar cell structures. In this work S.A, B and C are also expanded when we heated them [15]. By the help of change in lattice parameters, thermal expansion coefficients are calculated for symmetric (002), (004), (006) and (121) asymmetric planes. Lattice parameters according to the temperatures are given in table 7 for S.A, B and C.

Table 7(a). c- Lattice parameters in Å at different temperatures for S.A

hkl	*300 ºC*	*350 ºC*	*400 ºC*	*450 ºC*
(002)	5.305	5.282	5.373	5.267
(004)	5.293	5.283	5.295	5.277
(006)	5.287	5.284	5.288	5.280

Table 7(b). c- Lattice parameters in Å at different temperatures for S.B

hkl	*300 ºC*	*350 ºC*	*400 ºC*	*450 ºC*
(002)	5.306	5.310	5.327	5.315
(004)	5.313	5.314	5.321	5.316
(006)	5.316	5.316	5.318	5.316

Table 7(c). c- Lattice parameters in Å at different temperatures for S.C

hkl	*300 ºC*	*350 ºC*	*400 ºC*	*450 ºC*
(002)	5.283	5.289	5.2962	5.286
(004)	5.291	5.293	5.2958	5.291
(006)	5.293	5.295	5.295	5.294

Thermal expansion coefficients are calculated by using equations (7) and (8).

$$dl = l_0.\alpha.dT \quad (7)$$

here dl is the change in length with temperature difference, l_0 is the length before expansion, α is the thermal expansion coefficient and dT is the temperature difference causing expansion. If α is let alone in equation (7) formula giving thermal expansion coefficient is found. This formula is given in equation (8) [15].

$$\alpha = \frac{1}{l_0}\frac{dl}{dT} \quad (8)$$

Thermal expansion coefficients according to different planes are given in table 8.

This x4 difference in some thermal expansion coefficients are caused by volume defects.

For a more detailed explanation of differences in thermal expansion coefficients, shifts in peak positions are given in figure 4.

Table 8. Thermal expansion coefficients according to different planes for S.A, B and C

Plane	*α for S.A(1/ºC)(x10⁶)*	*α for S.B(1/ºC)(x10⁶)*	*α for S.C(1/ºC)(x10⁶)*
c-(002)	14.2	38.7	23.3
c-(004)	3.62	15.7	9.04
c-(006)	1.12	4.75	3.3
c-(121)	3.99	6.08	7.65
a-(121)	6.26	5.44	7.13

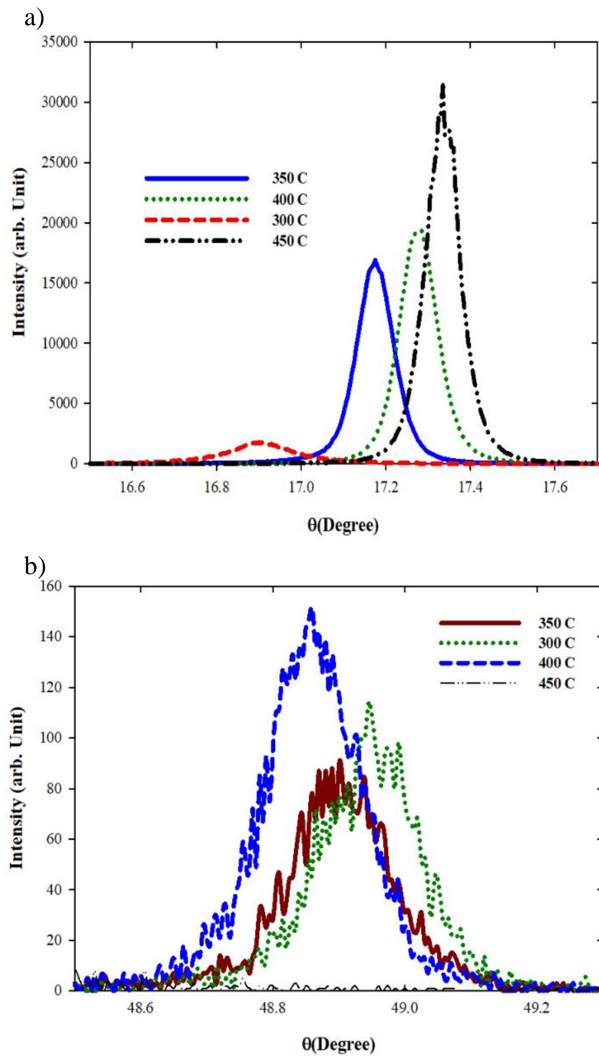

Figure 4. a) Shifts in peak positions of S.A for (002) symmetric plane b) Shifts in peak positions of S.C for (121) asymmetric plane

This figure shows the shifts in peak positions with an increase in temperature. These shifts cause differences in thermal expansion coefficients because when the lattice expands a- and c- lattice parameters change. In figure 4 shifts in peak positions are given for only symmetric (002) and asymmetric (121) planes as examples. In Figure 4 peaks are more separated from each for (002) plane if compared with (121) plane. This is the reason why thermal expansion coefficient is approximately 10 times larger than for (121) plane as can be seen in table 8. During the calculations of lattice parameters peak positions play an important role according to equations (3 and 4). Differences in thermal expansion coefficients for the same plane but for different samples can be used as the perfectly of the crystal structure forming solar cells and other devices formed by crystals. Imperfection might be occurred during growth.

4. CONCLUSION

In this study, structural properties of InGaN/GaN SCs are determined by HR-XRD technique. FWHM values of HR-XRD omega peaks are compared for GaN and InGaN layers individually. It is seen that FWHM values for GaN layers are nearly the same with each other for all three samples. FWHM values for InGaN layer in S.A is lower than S.B and C. This situation indicates that InGaN layer in S.A has a high crystal quality. When the plane mirror reflects the beam in diffraction angle, excellence of the plane maintains a correct pattern. This situations results in being high crystallite of the structure. In addition to this by using HR-XRD measurements, a- and c lattice parameters, strain and stress and crystal size are determined. Fault calculation is also made for lattice parameters. It is seen that fault percentage is not more than %2. During the calculation of lattice parameters cubic system is taken as reference for GaN layers and τ angle modification is used. For InGaN layer Vegard's law is employed. With the help of sinθ versus βcosθ plot crystal size and strain are calculated. The strain value ε_a obtained from this plot, elastic constants, Young modulus and Poisson's ratio are employed to calculate stress with two different methods and the results are compared whether they are in accordance or not. Finding different methods for all three samples is commented as the calibration shifts during growth of layers. Also, thermal expansion coefficients are calculated. Shifts in peak positions caused by increasing temperature are given. It is seen that thermal expansion coefficients found are in accordance with literature

REFERENCES

[1] Nakamura S., Pearton S., Fasol G., "The Blue Laser Diode", (2000).

[2] Davydov V.Y.; Klochikhin A.A.; Seisyan R. P.; Emtsev V.V.; Ivanov S.V.; Bechstedt F.; Furthmuller J.; Harima H.; Mudryi A.V.; Aderhold J.; Semchinova O.; Graul J., "Absorption and emission of hexagonal InN. Evidence of narrow fundamental band gap", ***Physica Status Solidi B-Basic Solid State Physics***, , 229 (3): R1-R3, (2002).

[3] Matsuoka T.; Okamoto H.; Nakao M.; Harima H.; Kurimoto E., "Optical bandgap energy of wurtzite InN", ***Appl Phys Lett***, 81 (7): 1246-1248, (2002).

[4] Green M. A.," Recent developments and future prospects for third generation and other advanced cells" ***Conference Record of the 2006 IEEE 4th World Conference on Photovoltaic Energy Conversion***, 1-2: 15-19, (2006).

[5] Luque A.; Marti A., "A Metallic Intermediate Band High Efficiency Solar Cell", ***Prog Photovoltaics***, 9: 73-86, (2001).

[6] Fetzer C. M.; King R. R.; Colter P. C.; Edmondson K. M.; Law D. C.; Stavrides A. P.; Yoon H.; Ermer J. H.; Romero M. J.; Karam N. H., "High-Efficiency Metamorphic Gainp/Gainas/Ge Solar Cells Grown by Movpe", ***J Cryst Growth***, 261: 341-348, (2004) .

[7] Law D. C.; Fetzer C. M.; King R. R.; Colter P. C.; Yoon H.; Isshiki T. D.; Edmondson K. M.; Haddad M.; Karam N. H., "Multijunction Solar Cells with Subcell Materials Highly Lattice-Mismatched to Germanium", ***Ieee Phot Spec Conf***, 575-578, (2005).

[8] Dridi Z.; Bouhafs B.; Ruterana P., "First-Principles Investigation of Lattice Constants and Bowing Parameters in Wurtzite Alxga1-Xn, Inxga1-Xn and Inxal1-Xn Alloys", ***Semicond Sci Tech***, 18: 850-856, (2003).

[9] Birks L. S. a. F., H.," Particle Size Determination from X-Ray Line Broadening", ***J Appl Phys***, 17: (1946).

[10] Delhez R.; Dekeijser T. H.; Mittemeijer E. J., "Determination of Crystallite Size and Lattice-Distortions through X-Ray-Diffraction Line-Profile Analysis - Recipes, Methods and Comments", ***Fresen Z Anal Chem***, 312: 1-16, (1982).

[11] Wassermann G. and G., J., "Texturen Metallischer Werkstoffe", (1962).

[12] Moram M. A.; Vickers M. E.," X-Ray Diffraction of Iii-Nitrides", ***Rep Prog Phys,*** 72, (2009).

[13] Kisielowski C., et al., "Strain-Related Phenomena in Gan Thin Films", ***Phys Rev B*** 54: 17745-17753, (1996).

[14] Suryanarayana C. a. N., M. G., "X-Ray Diffraction", (1996).

[15] Serway R. A. a. B., R. J. ," Physics for Scientists and Engineers", (2000).